University of Baghdad
College of Engineering
JE
JOURNAL OF ENGINEERING

Journal of Engineering

journal homepage: www.jcoeng.edu.iq

Volume 30 Number 6 June 2024

Experimental Study of Partial Open Side Effect on Natural Convection in a Porous Cavity

Mazin F. Fateh Ala[1,*], Raed G. Saihood[2]

Department of Mechanical Engineering, Collage of Engineering, University of Baghdad, Baghdad, Iraq
mazin.ali2003m@coeng.uobaghdad.edu.iq[1], Raed.hassan@coeng.uobaghdad.edu.iq[2]

ABSTRACT

This research provides information on the heat transfer in the cavity by natural convection which has a partially open side with a ratio (A = 1, 0.75, 0.5, 0.25) to the surroundings for cooling. It is filled with porous media (glass beads) and saturated with air. The bottom wall was heated with a constant heat flux (q = 1500, 3000, 4500, 6000) W/m^2 while the top and other walls of the cavity were well insulated. The porous media had small porosity (0.418), a range of Rayleigh number Ra (57.6-1470). The distribution of temperatures, the local Nusselt number, and the average Nusselt number were all extracted from the testing rig's temperature data. It is clear that the fluid flow and heat transfer are affected by heat flux and the ratio of partially open side. Observed that, the greatest temperature values at maximum heat flux (q) and minimum open ratio (A). Thus, the temperature rising at all values of the constant heat flux and the enhancement of the local Nusselt number at (q = 6000) W/m^2 about (5.47%, 3.85%, 1.76%) for (A = 1, 0.75, 0.5) respectively, when compared with (A = 0.25). The enhancement of the average Nusselt number at (q = 6000) W/m^2 is about (7.28%, 4.55%, 2.27%) for (A = 1, 0.75, 0.5) respectively, compared with (A = 0.25).

Keywords: Porous media, Natural convection, Partially open side, Cavity.

*Corresponding author
Peer review under the responsibility of University of Baghdad.
https://doi.org/10.31026/j.eng.2024.06.11

Article received: 13/07/2023
Article accepted: 29/09/2023
Article published: 01/06/2024

دراسة عملية لتأثير جانب مفتوح جزئيا على الحمل الحر في تجويف مسامي

مازن فؤاد فتح الله*، رائد كاطع صيهود

قسم الهندسة الميكانيكية، كلية الهندسة، جامعة بغداد، بغداد، العراق

الخلاصة

يقدم هذا البحث معلومات عن انتقال الحرارة في التجويف عن طريق الحمل الحراري الطبيعي الذي له جانب مفتوح جزئيًا بنسبة (A = 1، 0.75، 0.5، 0.25) إلى المحيط من أجل التبريد. التجويف مملوءة بمادة مسامية (خرزات زجاجية) مشبعة بالهواء. تم تسخين الجدار السفلي بتدفق حراري ثابت (q = 1500، 3000، 4500، 6000) واط / م^2 بينما تم عزل الجدار العلوي والجدران الأخرى للتجويف جيدًا. كان للمادة المسامية مسامية صغيرة (0.418)، مدى رقم رايلي Ra (57.6–1470). تم استخلاص كل من توزيع درجات الحرارة ورقم نسلت الموقعي ومتوسط رقم نسلت من بيانات درجة حرارة جهاز الاختبار. من الواضح أن تدفق الموائع ونقل الحرارة يتأثران بتدفق الحرارة ونسبة الجانب المفتوح جزئيًا. لوحظ أن أعلى درجة الحرارة عند الحد الأقصى لتدفق الحرارة (q) واقل نسبة للجانب المفتوح (A). وبالتالي، ترتفع درجة الحرارة عند جميع قيم التدفق الحراري الثابت ويتحسن رقم نسلت الموقعي عند (q = 6000) وات / م^2 حوالي (5.47٪، 3.85٪، 1.76٪) لـ (A = 1، 0.75، 0.5) على التوالي، عند المقارنة بـ (A = 0.25). زيادة متوسط رقم نسلت عند (q = 6000) واط / م^2 حوالي (7.28٪، 4.55٪، 2.27٪) لـ (A = 1، 0.75، 0.5) على التوالي، مقارنة بـ (A = 0.25).

الكلمات المفتاحية: الوسط المسامي، الحمل الحر، جانب مفتوح جزئيا، تجويف.

1. INTRODUCTION

Recent research attempts to improve heat transmission in many energy sources, such as renewable energy (geothermal, wind, and solar), have benefited from the application of the porous media approach **(Kaviany, 1995)**. Researchers have shown a great deal of interest in porous media's impacts, particularly during the past 40 years because of how frequently it is used in environmental and practical applications due to its low cost **(Vafai, 2015)**. Many applications used porous media such as the development of oil and natural gas making from reservoir and growth crowd oil – shale **(Straughan, 2008)** and fresh the soil by steam injection and ecological ground (soil) water population **(Nield and Bejan, 2017)**, elimination of pollution through water-filled ground, soil transference in groundwater **(Ingham, 2005)**, treatment of sewage, fruit storage, grain drying, dehydration, drying, and processing facilities **(Koua et al., 2019)**.

A numerical and experimental investigation for free convection in a straight-up rectangular cavity with a porous layer was investigated by **(Beckermann et al., 1987; Beckermann et al., 1988)**. The numerical model was performed utilizing the Brinkman–Forchheimer–extended Darcy equations. In experiments, the enclosure was conducted with spherical glass beads filled by water and glycerin. Thermostats and a Mach-Zehnder interferometer were utilized to visualize the temperature and flow shapes. They found that the liquid transportation from the free region to the porous region proportional directly with Darcy (Da) and Rayleigh (Ra) numbers. For low Ra-Da numbers, the flow circulates primarily in the free portion, and the conduction is the permanent manner for heat transfer in the porous

region. The initiation of convection caused by warming from below was explored by **(Chen et al., 1991)** in a cavity partially filled with anisotropy permeability and thermal diffusivity porous layer. It is found that the influence of anisotropic on the initiation of heat convection is strongest for low amounts of depth ratios. Reduced vertical permeability in a porous media stabilizes the arrangement of superimposed layers, and heat is largely transported via the porous region by conduction.

The influences of the Ra, thickness ratio, and aspect ratio on convection were studied by **(Kim and Choi, 1996)** in a cavity partially filled with a porous layer which is heated at the bottom surface. They found that heat transfer varies intensely due to the influence of the aspect ratio and the matching cells when the depth ratio is 0.1. Underground dangerous waste and other hygroscopic farming products, a model was used by **(Prakash et al., 1999)** to expect hydrothermal properties in a system with a turbulent flow over a saturated hygroscopic porous media. Experimental data was compared with the numerical simulation to verify the accuracy of this model. A special case using silica gel was simulated to demonstrate how the model could be used. **(Pal et al., 2006)** calculated the permeability coefficient of porous media using Parker Print Surf porosity and Darcy's equation. It may be utilized to rank porous layers in terms of fluid preoccupation and scattering rate, estimate pore size, and predict the coating thickness needed. It can also be used to predict how well a porous medium would function as a barrier. **(Mahdi et al., 2006)** numerically investigated the thermophysical phenomenon of natural convection in a porous cavity. They found that porous Ra and cavity geometry possess an important impact on thermal performance. **(Sathiyamoorthy et al., 2007)** examined natural convection flows in a square enclosure with a porous media. The penalty finite element technique and the Darcy-Forchheimer model are utilized to simulate the transfer of momentum. Numerical results are reported for various factors, including Rayleigh, Darcy, and Prandtl numbers. At Da = 10^{-5}, they discovered that the mean Nusselt numbers did not vary at Ra up to 10^6, this is because the conduction mode is permanent in heat transfer but in general the mean Nusselt number rises with the augment of Da and Ra.

(Yoon et al., 2009) examined the effect of the interior cylinder placement on heat transmission and fluid flow. Natural convection splits into an unsteady and steady state when the interior circular cylinder is moved vertically along the square cavity's midline. At an inner cylinder location greater than 0.18, a shallow layer forms between its upper surface and the upper surface of the cavity, creating alternate upwelling and downwelling plums. Additionally, modifications in the transfer of heat quantities have been shown. **(Hussain and Hussein, 2010)** also examined the effect of a warm inner circular cylinder on a square air cavity. The Rayleigh numbers were modified from (10^3) to (10^6). Low Ra had a slight influence on the flow field, while large Ra had a major influence. The numerical data produced a double-cellular flow field, and the average Nusselt number exhibits nonlinear behavior with respect to position. Streamlines, isotherms, local Nusselt numbers, and average Nusselt numbers were used to present the results. They found that Nu improved when the inner cylinder moved away from the center. The one-domain version of the conservation equations was used by **(Bagchi and Kulacki, 2011)** to describe free convection in a porous cavity with constant hot temperature at the lower surface. The influence of many parameters on Nu was investigated. Nusselt numbers increased by decreasing the heater size and height ratio and raising Da. Increases in Da and Nu were correlated with declines in the heater's ratio, while a rise in Rayleigh number was associated with complex flow reorganization.

(Yazdchi et al., 2011) used the Finite Element Method to study crosswise permeability for creeping flow across unidirectional arbitrary arrangements of fibers/cylinders. A modified Carman-Kozeny (CK) relation was provided, which is true over a wide range of porosities. This connection could be used to make composite materials and validate coarse models of particle-fluid interactions. FlexPDE student version 6.17 was used by **(Khansila and Witayangkurn, 2012)** to compute the free convection visualization in a porous cavity heated by sinusoidal temperature on the left side. Isotherms, streamlines, and heat lines were used to display the results, with two circulations present inside the cage for the streamlines. Rayleigh and Darcy's numbers raised along with the values of streamlines and heat lines. Also, **(Kalaoka and Witayangkurn, 2012)** used FlexPDE 6.14 student version to examine free convection mode in a square porous container. Many variables such as Da, Gr, Pr, and Re were solved and the outcomes were represented using isotherms, streamlines, and headlines. As Darcy and Grashof's numbers rise, fluid motion strength, streamlined magnitudes, and temperature distribution all change. **(Mehdy, 2012)** numerically investigated the thermophysical phenomenon of natural convection in a porous cavity. He found that buoyancy ratio and porous media properties possess an important impact on thermal performance.

Core flooding experiments were conducted by **(Lock et al., 2012)** to test the permeability of porous media in the laminar region at the basic flow rate. The progression of the flow regimes was charted using the permeability versus flow rate plot, but this presents difficulties when tracking the change from laminar to turbulent regimes. **(Hussein, 2013)** used a finite volume computer model of free convection to solve an air-filled parallelogrammical cavity with a heating concentric cylinder. The findings demonstrated that as Ra rises, the force of circulation and thermal boundary layer thickness about the heated cylinder both increase significantly. To increase flow circulation, the location of the inner cylinder might be lowered until it reaches 0.2 m from the center and the parallelogrammical chamber sides should be tilted at 15°. **(Mashkour et al., 2013)** used experimental methods to study heat transmission in a porous media. A saturated porous glass medium with dimensions of (30 × 30 × 30) cm was placed within the box. A heater was utilized to warm the box's lowest wall; the remaining walls were thermally isolated. For five different heat flux values (348, 576, 839, 1147, and 1384W/m^2), the influence of a porous material on natural convection heat transfer was examined. The findings indicated that as Ra increases, the temperature inside space increases.

(Hussain and Raheem, 2013) investigated the thermophysical processes along a wall in a porous material which is thermally stable. The temperature distribution and Nusselt number were studied statistically and empirically. Results showed that the distribution of temperature is significantly affected by thermal stratification, rising as thermal stratification falls, but not significantly by inclination angles. The Nusselt number increases with decreasing stratification parameters and changes linearly with the downstream coordinate. The finite Element Method was used by **(Hatami and Safari, 2016)** to investigate the free convective transfer of heat of nanofluids in a wavy-wall cavity. Temperatures, streamlines, and contours of concentration could be changed by moving the cylinder in the X and Y directions. Results showed that both wavy side walls' heat transfer is aided by the cylinder's center placement. Alumina fibers and hollow silica powders were used by **(Xu et al., 2017)** to create a unique ceramic composite insulation material (CCIM). Microstructure analysis and thermal conductivity testing showed that the fabricated CCIMs have significantly lower thermal conductivity than conventional mineral wool. Surface temperature and surface heat

flux measurements showed superior insulation capabilities than conventional inorganic insulation materials.

Oil shale is an organic-rich mudstone with low porosity and low permeability before it is converted into oil and gas. When lithostatic loads confine fracture permeability, permeabilities only rise to the milli-Darcy level. The increase in permeability is connected to a rise in both porosity and pore diameter **(Burnham, 2017)**. The theoretical and experimental study was investigated by **(Hussain and Luma, 2018)** for free convection via a cubic hollow was authorized. Rayleigh numbers and angles of inclination demonstrated the influence of these variables on the temperature profile. The results of the experiment and numerical analysis were compared, and it was found that the temperature distribution and Nu exhibit identical trends but are approximate with mean differences of 11.5% and 15.6% respectively. The shrinkage, density, porosity, heat, and mass transfer parameters of cocoa beans were investigated during indirect sun drying by **(Koua et al., 2019)**. They found that shrinkage and porosity rise when the moisture content is lowered. The effective moisture diffusivity ranged from (5.49×10^{-10}) to (4.26×10^{-10}) m^2/s.

Hydrothermal data was collected and correlated. Rayleigh-Bénard convection was studied experimentally by **(Ataei-Dadavi et al., 2019)** in an enclosure filled with solid spheres. Nusselt numbers were measured using Rayleigh number range between 10^7 and 10^9. Particle picture velocimetry and liquid-crystal thermal imaging were used to highly acquire resolution temperatures and velocity fields. The results showed that the asymptotic regime's velocity magnitudes were significantly higher than the lower Rayleigh number regimes due to more efficient heat transfer. **(Abdulsahib and Al-Farhany, 2020)** examined the combined convective in a square container divided into two layers: an upper layer of an Al_2O_3-water Nanofluid and a bottom layer of a porous medium. The temperature distribution was measured using 15 thermocouples and a thermal imaging camera at concentrations of nanoparticles, temperature differences between the cold and hot sides, and angular velocities. The results showed that the distribution of temperature was even along the top portion of the cavity, while the lower half was constrained near the hot wall zone.

The numerical analysis of a porous cavity with saturation fluid and natural convection was done by **(Mohammed and Ali, 2021)** using the finite element method. The findings showed that varying the heaters' positions had a limited impact on boosting free convection. The mean Nusselt number increased by 9% at the lower heater, while it declined by 5.6% at the top heater. The local Nu magnitude was highest at the cavity's middle length. **(Hussein and Ali, 2023)** investigated numerically two-dimensional in-nature unstable mixed convective in a porous cavity heated from the bottom plane. The Darcy model was utilized to simulate fluid flow and the combined impacts of pressure and temperature are examined. It had been discovered that when pressure head and heat flux rise, the time needed to obtain a favorite temperature at the bottom wall decreases, keeping wider areas close to the upper wall at lower temperatures.

(Zachi and Ali, 2023) examined the heat transfer caused by free convection in a square cavity with a dimension of 20 cm, saturated porous material, and free air filling the remaining space. Porous layer with a thickness of (2.5, 5, 7.5, and 10) cm and heater sizes of (20, 14, and 7) cm were used in the experiments. The results showed that the thermophysical properties are influenced by the porous layer thickness and are at their maximum at 0.25L of porous layer thickness with a greater heater length (20 cm) and higher heat flux (q=600 W/m^2). The mean heat transfer improvement is more significant for bigger heater sizes as the effect of increased heater length becomes more pronounced. **(Kamal and Saihood, 2024)** investigated numerically the effect of open walls on free convection in a porous cavity.

The cavity was heated from below and its one vertical wall, opposite to the open wall, was maintained at a cold temperature. They found that heat transfer performance increases with permeability increase.
In general, the porous enclosure with a partially open side has lacked interest, especially for experimental research. So, in the present experimental work, the steady free convective in the cavity was heated from the lower plane by uniform heat flux and cooled by opening one side wall to the environment and insulating the top and remaining walls.

2. EXPERIMENTAL SETUP

The present work consists of a partially open cavity. **Fig. 1** shows the schematic diagram of the test rig. The test section is a cubic cavity with constant length (L = 20 cm) while the open part (H) varies from 20 cm to 5 cm, A (1 – 0.25). This cavity is fully filled with porous media, (2.4-2.9) mm glass beads, saturated with air. The heating source is in the bottom plate with uniform heat flux and the partially open right wall represents the natural heat sink to cool this cavity while the other walls are well insulated. The open side is covered with a metal grid to prevent the glass beads from escaping from the cavity and allowing air to penetrate it to cool the cavity from the surrounding temperature (Tc). The ranges of investigated parameters in the present work are listed in **Table 1. Table 2** shows the thermophysical characteristics of porous media and air **(Bejan and Kraus, 2003)**. **Table 3** shows the device specifications.

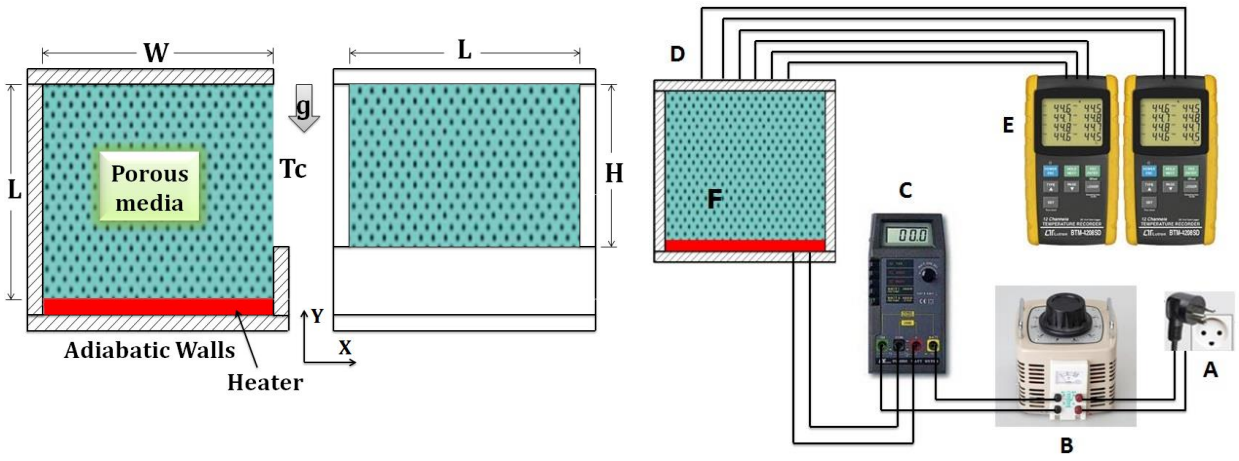

Figure 1. The schematic diagram of the experimental work (Left) The physical geometry of the problem (Right) Schematic diagram of the test rig; (A) Power Source, (B) Variac, (C) Wattmeter, (D) Thermocouples, (E) Data Logger, (F) Test Section.

Table 1. The variable values for experimental work.

Parameter	Values
Width of Cavity (H)	(20,15,10,5) cm
Aspect Ratio (AR=W/L)	(1,0.75,0.5,0.25)
Heat Flux (q)	(1500,3000,4500,6000) (W/m^2)
Porosity (ε)	0.418
Time of testing	(12:00 - 8:00) PM

Table 2. Thermophysical characteristics of porous media and air.

Physical properties	Air	Glass Beads
Density (kg/m^3)	0.98	2510.72
Heat Capacity (J/kg.K)	1007	671
Thermal Conductivity (W/m.K)	0.031	0.871

Table 3. The device's specifications

Device	Model	Specification
Variac	R52-260H	Input=220V Output=0-260V, Capacity=2000VA
Wattmeter	DW-6060	AC power: 2000W,6000W (±1%) Input Voltage: (0 - 600) ACV (±0.8%) Input Current: (0 - 10) ACA (±1%) Frequency: (45 - 65) Hz
Data Logger	BMT-4208 SD	12 channels Temperature recorder Sensor type: Type J/K/T/E/R/S thermocouple Type K thermometer: (-100 to 1300) ℃

2.1 The Porous Media Properties

The porous media is an arrangement of a solid matrix with fluid-filled gaps (air). The glass beads utilized as the solid matrix in this study were spherical, and they were evaluated and quantified using the following system:

2.1.1 Glass Sphere Diameter (d)

Twenty-four glass spheres were randomly selected and micrometer-measured to comparation the dimensions of utilized glass beads (Type-S) manufactured of soda-lime glass with the information sheet production. The standard size (4510) of the supplier's standard sizes, which range from (2.40 to 2.90) mm, was determined to have an average diameter of (2.6566) mm.

2.1.2 The Porosity (ε) Measurement

Experimentally established mean porosity of glass beads was determined by dividing the volume of water that saturated with glass beads by the entire volume of the cavity containing the beads and fluid according to Eq. (1), as shown below:

$$Porosity\ (\varepsilon) = \frac{Fluid\ Volume}{Total\ Volume} = 1 - \frac{Solid\ Volume}{Total\ Volume} \quad (1)$$

At (25) °C room temperature, the estimated average magnitude for the porosity of glass beads (ε) was found to be (0.418).

2.1.3 The Density Measurement

To evaluate the glass beads density involved in production of material certificates, an experimental test was used to determine it. This involves weighting a sample of glass beads

to determine its total weight then determining its volume from addition water in a measuring cylinder (water displacement method) and determining its mean volume from the alteration between the two readings (glass beads with water and water only). Next, the average density of the beads is determined by dividing the weight of glass beads over its volume. Finally, determining whether the average density is within the acceptable range from the data sheet of the manufacture of material certificates with different percentage (3.7%).

2.1.4 Permeability

The capacity of fluid to flow via channels created by porous media voids is known as permeability, which is a critical macroscopic feature of porous media. The porous media's solid matrix component shape and manner of creation have the most significant effects on permeability calculations. As a consequence, a number of models, including the packed sphere model, the loads of capillary gaps model, and the bundle of capillary tubes model, were used to determine the findings. **(Kaviany, 1995; Yazdchi et al., 2011; Mohammed and Ali, 2021)**. Due to the impacts of large compressibility, adsorption, and slippage, determining the value of permeability, especially for gas, requires a difficult test compared to liquid. With low pressure and a high Da, the impacts of the slippage will be exacerbated. Water flow at laminar was used in the current study to fastest the calculation process while ignoring the impact of slippage and adsorption on the experiments. As a result, the flow field is the major parameter affecting permeability that is due to the laminar flow which causes the pressure drop to be linearly related to the fluid flow **(Bejan and Kraus, 2003)**. Henry Darcy (1856) further developed it into Eq. (2), which is dependent on fluid discharge (flow rate), fluid dynamic viscosity, and pressure gradients in the direction of flow in a porous media.

$$\mathrm{K} = \frac{\boldsymbol{\varepsilon^3 d^2}}{\boldsymbol{180(1-\varepsilon)^2}} \tag{2}$$

The experimental process for estimating permeability is shown in **Fig. 2.** First, the tank was filled with distilled water at a constant head and sphere-shaped glass beads was arranged in a pipe. Then, water was allowed to flow through the pipe and the amount of water that is discharged through the porous material in the test section was collected in a scalar cylinder with stopwatch to compute the water discharge. Darcy's law was used to compute permeability by Eq. (3) **(Hussain and Raheem, 2013; Zachi and Ali, 2023)**:

$$\mathrm{Qwater} = \frac{\boldsymbol{K}}{\boldsymbol{\mu_f}}\left(\frac{\boldsymbol{\triangle p}}{\boldsymbol{L}}\right)\boldsymbol{A} \tag{3}$$

where, Qwater is the Water discharge through porous media, (m^3/sec).
A is the Cross-section area of the porous media, (m^2).
μ_f is the Dynamic viscosity of fluid, (kg/m.s).
L is the Enclosure dimension, (m).
$\triangle p$ is the Pressure gradient, (Pa).
Other properties such as thermal conductivity and heat capacity depended on **(Zachi and Ali, 2023)** for the porous media, and effective thermal conductivity and heat capacity are computed from Eq. (4) and Eq. (5) **(Nield and Bejan, 2017)**.

$$K_{eff} = (1-\varepsilon)k_s + \varepsilon k_f \quad (4)$$
$$cp_{eff} = (1-\varepsilon)cp_s + \varepsilon cp_f \quad (5)$$

where, k_f is the fluid's thermal conductivity for air (W/m. K).
k_s is the solid's thermal conductivity for glass beads (W/m. K).
K_{eff} is the effective thermal conductivity of the porous region (W/m. K).
cp_f is the specific heat capacity of the fluid for air (J/ kg.K).
cp_s is the specific heat capacity of the solid for glass beads (J/ kg.K).
$cp_{eff}$is the effective specific heat capacity of the porous medium (J/ kg.K).

The average physical properties of the glass beads that were used in this study are listed in **Table 4.**

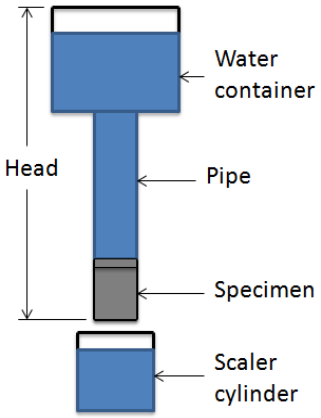

Figure 2. Permeability Test Rig

Table 4. Characteristics of the Porous Matrix

Property	Value
Permeability	$1.61*10^{-9}$ (m^2)
Porosity	0.418
Density	2515.81(kg/m^3)
Thermal conductivity	1.072054 (W/m.K)
Specific capacity	1329 (J/kg.K)

2.2 Experimental Procedure

2.2.1 Temperature Measurement

The distribution of the thermocouples as shown in **Fig. 3**, five thermocouples were dispersed along the bottom center line of the cavity to measure the mean temperature on the hot surface, using 20 thermocouples to record the distributed temperature in a mid-plane at various heights above the floor. To ensure the symmetry of the system, ten thermocouples were dispersed in two vertical plane groups at various points as shown in **Fig. 3**, it's in two sides of the center thermocouple grid. In order to compare the data with the output of a

temperature indicator (an electronic device called an elcometer), two thermocouples were employed to measure the temperature on the side and bottom of the cavity at the exterior surface of the insulation. Two methods are used to gauge the surrounding temperature, an elcometer and a thermocouple mounted close to the rig. Before beginning the experimental work, every thermocouple equipped with a data logger has been examined and calibrated.

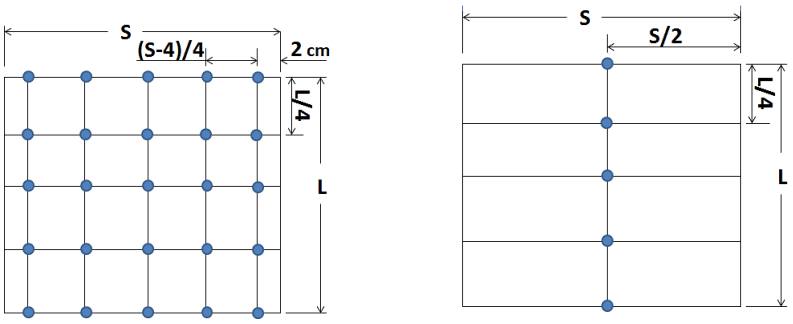

Figure 3. Thermocouples Grid Inside the Cavity (Left) Major Grid (Right)Two-Side Grid

2.2.2 Experiment Method

The average recorders of air temperature have been used to lessen the temperature influences of the environment on test outcomes. Choosing a location for the rig that is away from sunlight, air moving, vibration, and other factors will help to limit its volatility. An experiment process, place the thermocouple where it is supposed to be and fillings the cavity (test portion) with glass beads then turn on the power switch to allow voltage to flow through the Variac and set it to the proper volts, turn on an electric heater and use a wattmeter to adjust the power until it produces the appropriate constant heat flux (q = 1500, 3000, 4500, 6000) W/m^2, wait until the data logger measures stability, which takes between (8-12) hours depending on the aspect ratio of open part (A = 1, 0.75, 0.5, 0.25), all thermocouple temperature data should be noted and saved, shut down the power, and wait while the temperature is equal to room's temperature (use a cooling fan to hasten the temperature drop). Repeat the earlier experimental procedure for the various open ratios of the cavity (A = H/L = 1, 0.75, 0.5, 0.25).

3. THE RESULTS AND DISCUSSIONS

3.1. Temperature Distribution

The present work was illustrated the results of analyzing the natural convection of the cavity has a various open aspect ratio (A = 1, 0.75, 0.5, 0.25) which is filled with porous media (glass beads) saturated with (air) and heated from the lower wall by uniform heat flux (q) for cases (1500,3000,4500,6000) W/m^2. The porous media has a small porosity (ε = 0.418), and a range of Rayleigh number Ra (57.6 - 1470). The data of experimental work were recorded by a grid of distributed thermocouples to shelter the whole cavity. **Fig. 4** shows the distributed temperature for each case of the open aspect ratios. An increase in heat flux (q) leads to increases in the energy entering the system, which increases the temperature of the system, so the relationship between them is direct. While the decrease in ratio of the partially open side caused to increase the temperatures inside the system because of the small side

opening to heat exchange with the surroundings for cooling. Observed the temperature variation at the heater surface is due to the generation of air eddy currents under the influence of the partially open side, and the greatest temperature values recorded at heat flux (q = 6000) W/m^2 and a ratio (A = 0.25).

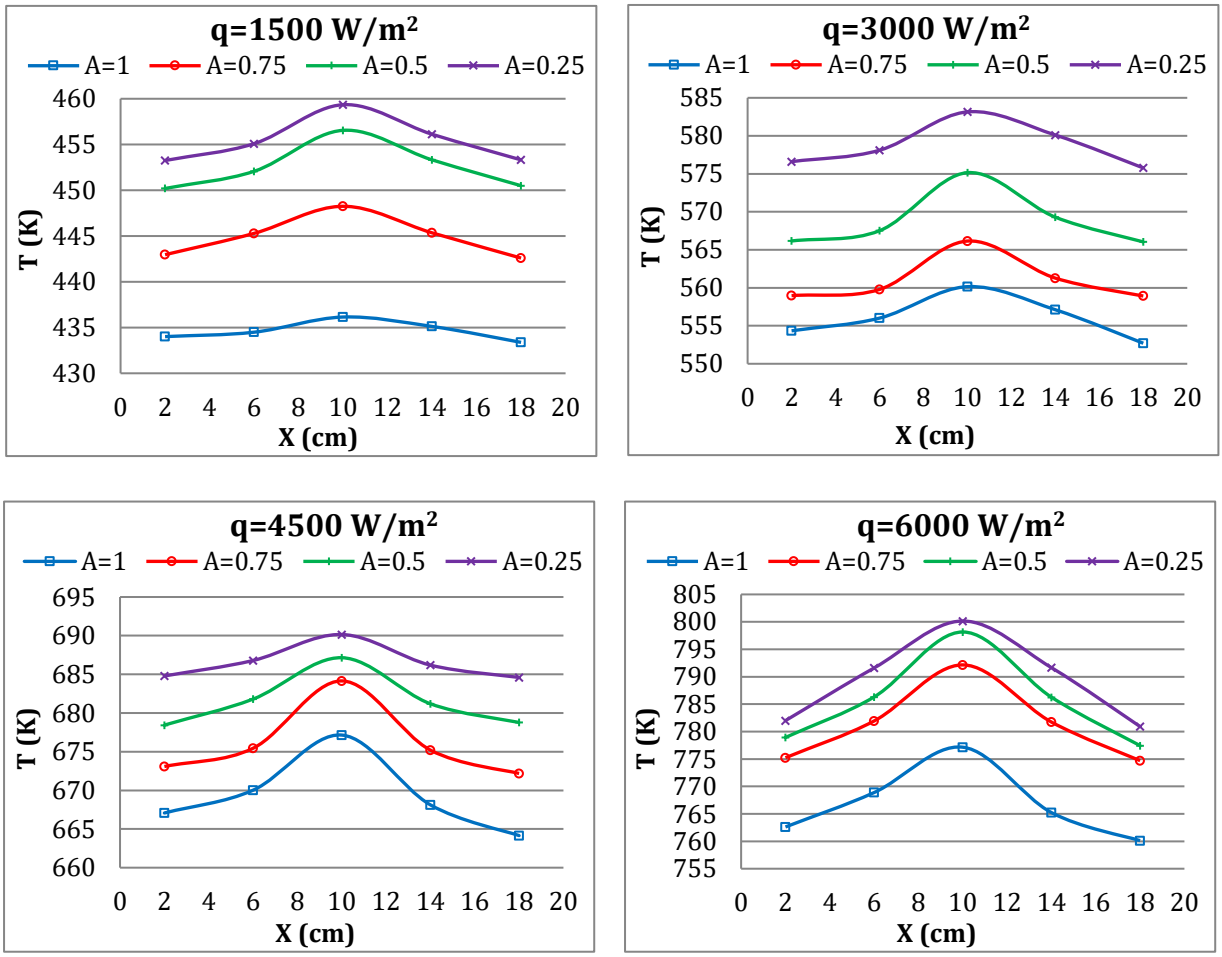

Figure 4. Temperature Distribution of Experimental Work with X-axis, for the Various Aspect Ratios

3.2. The Local Nusselt Number

The local Nusselt number (Nu) on the heated wall of the cavity was calculated by Eq. (5).

$$Nu = \frac{heat\ transfer\ by\ covection}{heat\ transfer\ by\ conduction} = \frac{h_x X}{k_f} \quad (5)$$

where, h is the heat transfer coefficient (W/m^2. K), X is the length of the heated surface (m). The heat transmission inside the cavity was dominated by convection or conduction mode and studying the effect of different parameters on heat transferred in the various open ratios, the local Nu is calculated for the constant heat flux range. For all cases, due to the growth in the energy quantities that are established from the bottom, that drives the heat transferred by convective is larger than conductive mode, the local Nusselt number raises with heat flow downstream of heated surface coordinates (x), according to the Eq. (5). The effect of increasing the flow rate of air at the partially open side of the cavity leads to a rise in

convection. **Fig. 5.** shows that the increase in heat flux (q) causes an augment in Ra value, and thus the Nu increases significantly at heat flux (q = 6000) W/m², and the extension in the open part causes an augment in the Nusselt number.

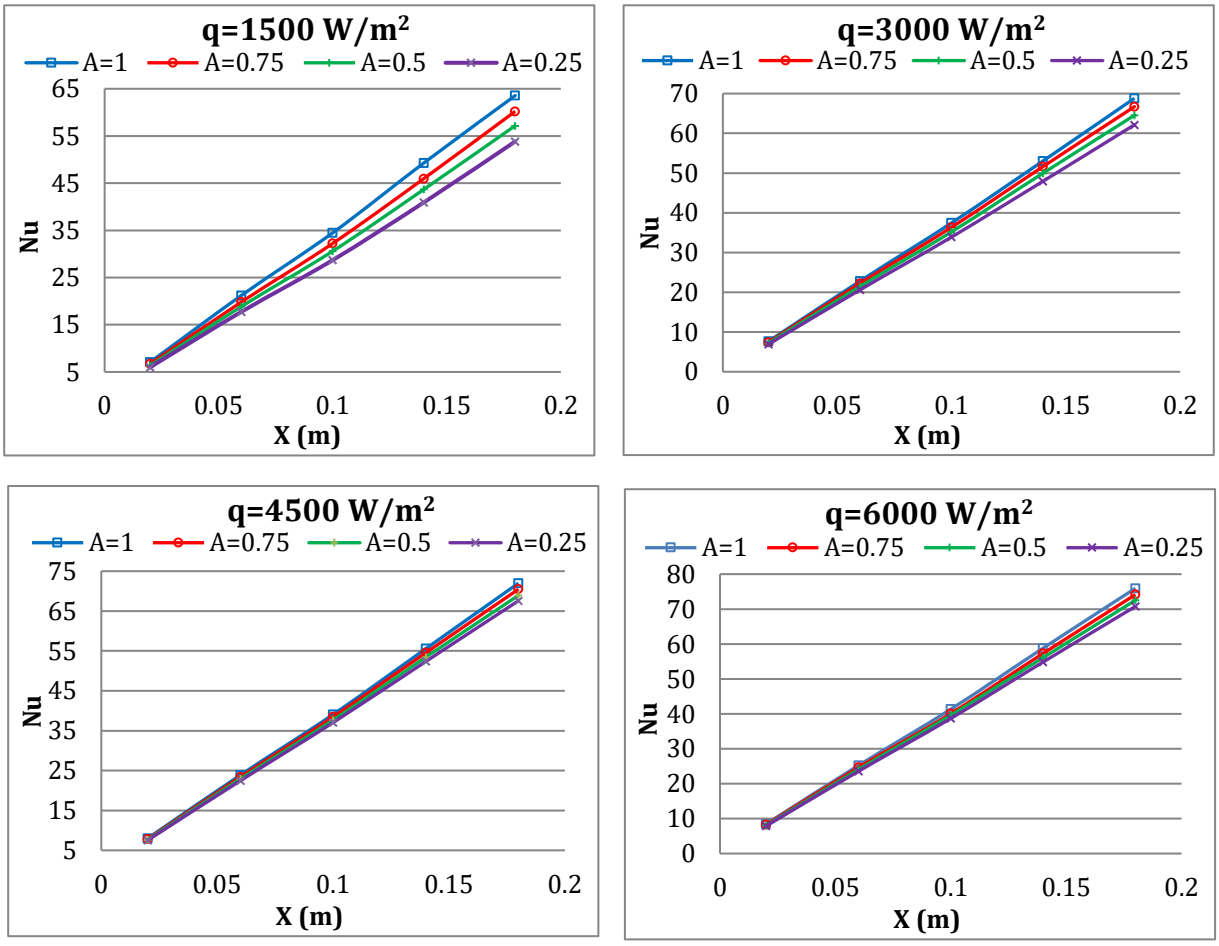

Figure 5. Relationship the Local Nusselt Number with Aspect Ratio at Constant Heat Flux for the Various Aspect Ratios.

Thus, the greatest value at (A = 1), because of increase the exchange area for heat transfer with the surrounding. The enhancement of the local Nusselt number at (q = 6000) W/m² is about (5.47%, 3.85%, 1.76%) for (A = 1, 0.75, 0.5) respectively, when compared with (A=0.25). While the percentage of increasing in the local Nusselt number when rises from (q = 1500) W/m² to (q = 6000) W/m² for the four open ratios as follows (20.1%, 24.58%, 29.68%, 35.04%) at a ratio (A = 1, 0.75, 0.5, 0.25) respectively.

3.3. Average Nusselt Number

The mean Nusselt number is calculating by integrating the local Nusselt number and plot with heat flux.

$$\mathrm{Nu}_{avg} = \frac{1}{L}\int_0^L \mathrm{Nu}\, dy \qquad (6)$$

Fig. 6 illustrates that the mean Nu increased by increasing in heat flux and increases more with a ratio of the partially open side (A = 1) due to augment the portion of porous region exposure to the surrounding for cooling, thus leading to increasing convective heat transfer. For the heat transfer enhancement to be maximum must be the ratio of the open side (A = 1), and it decreases to minimum value with decreasing aspect ratio to (A = 0.25). The development of the average Nusselt number at (q = 6000) W/m^2 for the aspect ratio (AR = 1, 0.75, 0.5) is about (7.28%, 4.55%, 2.27%), (9.6%, 5.3%, 3.1%), and (12.21%, 5.74%, 3.43%) for (A = 1, 0.75, 0.5) respectively, compared with (A = 0.25).

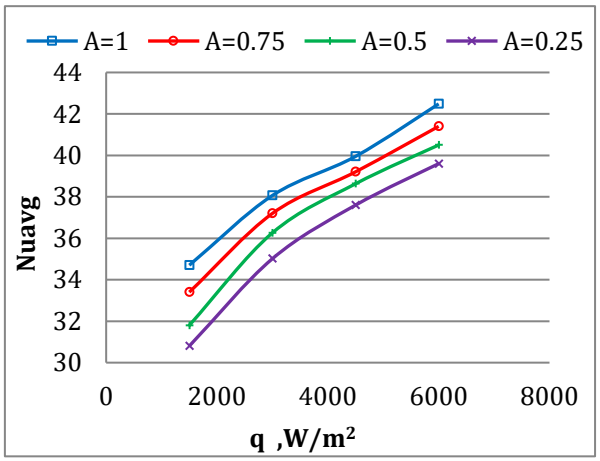

Figure 6. Relationship the Average Nusselt Number with open Ratio and Heat Flux.

4. CONCLUSIONS

The purpose of the article was to investigate free convection in a porous cavity with open side, heated from the lower wall by a uniform heat flux (q) of (1500, 3000, 4500, 6000) W/m^2, and cooled from the partially open side with a ratio (A) of (1, 0.75, 0.5, 0.25), cooling to the ambient, to find the best case of heat transfer by increasing Nusselt number, where significant results as shown in below:

1. The distribution of temperature in the cavity is affected by the ratio of the partially open side, the temperature of the heater surface rising at all heat flux values for the various open ratios.

2. The increase in a ratio of partially open side (A) of (1, 0.75, 0.5) affected the enhancement of the local Nusselt number at all values of the heat flux for the various aspect ratios (AR) of (1, 0.75, 0.5) when compared with (A of 0.25).

3. The heat flux value affected the increase in the local Nusselt number when rises from (q=1500) W/m^2 to (q of 6000) W/m^2 as follows (20.1%, 24.58%, 29.68%, 35.04%), at a ratio (A) of (1, 0.75, 0.5, 0.25) respectively.

4. The increase in the ratio of partially open side effects the augmentation of the average Nusselt number at (q of 6000) W/m^2 about (7.28%, 4.55%, 2.27%) for (A) of (1, 0.75, 0.5) respectively, compared with (A of 0.25).

NOMENCLATURE

Symbol	Description	Symbol	Description
A	Open aspect ratio	L	Length, m
AR	Aspect ratio	Nu	Local Nusselt number
cp_{eff}	Effective specific heat capacity, J/Kg.K	$Nu_{avg.}$	Average Nusselt number
cp_f	Fluid's specific heat capacity, J/Kg.K	p	Pressure, N/m^2
cp_s	Solid's specific heat capacity, J/Kg.K	q	Heat flux, W/m^2
d	Glass beads diameter, m	Ra	Rayleigh number
Da	Darcy number	T	Air temperature, °C
H	Open side height, m	x	Dimensional length of the x-axis, m
h_x	Heat transfer coefficient, W/m^2. K	ρ_{air}	Air density, kg/m^3
K	Porous permeability, m^2	Δ	Difference between two values
k_{eff}	Effective thermal conductivity, W/ (m.K)	ε	Porosity
k_f	Fluid's thermal conductivity, W/ (m.K)	μ_f	Fluid dynamic viscosity, kg.m/s
k_s	Solid's thermal conductivity, W/ (m.K)		

Credit Authorship Contribution Statement

Mazin F. Fateh Ala: Writing – review & editing, Writing – original draft, Experimental work. Raed G. Saihood: Writing – review & editing, Methodology.

Declaration of Competing Interest

The authors declare that they have no known competing financial interests or personal relationships that could have appeared to influence the work reported in this paper.

REFERENCES

Abdulsahib, A.D. and Al-Farhany, K., 2020. Experimental investigation of mixed convection on a rotating circular cylinder in a cavity filled with nanofluid and porous media. *Al-Qadisiyah Journal for Engineering Sciences, 13(2), pp. 99–108*. Doi:10.30772/qjes.v13i2.653.

Ataei-Dadavi, I., Chakkingal, M., Kenjeres, S., Kleijn, C.R. and Tummers, M.J., 2019. Flow and heat transfer measurements in natural convection in coarse-grained porous media. *International Journal of Heat and Mass Transfer, 130, pp.575–584*. Doi:10.1016/J.IJHEATMASSTRANSFER.2018.10.118.

Bagchi, A. and Kulacki, F.A., 2011. Natural convection in fluid–superposed porous layers heated locally from below. *International Journal of Heat and Mass Transfer, 54(15–16), pp. 3672–3682*. Doi:10.1016/j.ijheatmasstransfer.2011.01.034.

Beckermann, C., Ramadhyani, S. and Viskanta, R., 1987. Natural convection flow and heat transfer between a fluid layer and a porous layer inside a rectangular enclosure. *Journal of Heat Transfer, 109(2), pp. 363–370.* Doi:10.1115/1.3248089.

Beckermann, C., Viskanta, R. and Ramadhyani, S., 1988. Natural convection in vertical enclosures containing simultaneously fluid and porous layers. *Journal of Fluid Mechanics, 186, pp. 257–284*. Doi:10.1017/S0022112088000138.

Bejan, A. and Kraus, A.D., 2003. *Heat transfer handbook. J. Wiley*.

Burnham, A.K., 2017. Porosity and permeability of Green River oil shale and their changes during retorting. *Fuel, 203, pp. 208–213*. Doi:10.1016/J.FUEL.2017.04.119.

Chen, F., Chen, C.F. and Pearlstein, A.J., 1991. Convective instability in superposed fluid and anisotropic porous layers. *Physics of Fluids A: Fluid Dynamics, 3(4), pp. 556–565.* Doi:10.1063/1.858117.

Hatami, M. and Safari, H., 2016. Effect of inside heated cylinder on the natural convection heat transfer of nanofluids in a wavy-wall enclosure. *International Journal of Heat and Mass Transfer, 103, pp. 1053–1057*. Doi:10.1016/J.IJHEATMASSTRANSFER.2016.08.029.

Hussain Ehab, S. and Luma Ali, F., 2018. Natural convective heat transfer in an inclined open porous cavity with non-uniformly heated wall. *Association of Arab Universities Journal of Engineering Sciences, 25(5), pp. 529–547*.

Hussain, I.Y. and Raheem, B.K., 2013. Natural convection heat transfer from a plane wall to thermally stratified porous media. *International Journal of Computer Applications, 65(1), pp. 42–49.*

Hussain, S.H. and Hussein, A.K., 2010. Numerical investigation of natural convection phenomena in a uniformly heated circular cylinder immersed in square enclosure filled with air at different vertical locations. *International Communications in Heat and Mass Transfer, 37(8), pp. 1115–1126*. Doi:10.1016/J.ICHEATMASSTRANSFER.2010.05.016.

Hussein, A.K., 2013. Computational analysis of natural convection in a parallelogrammic cavity with a hot concentric circular cylinder moving at different vertical locations. *International Communications in Heat and Mass Transfer, 46, pp. 126–133*. Doi:10.1016/J.ICHEATMASSTRANSFER.2013.05.008.

Hussein, I.Y. and Ali, L.F., 2023. Mixed convection in a square cavity filled with porous medium with bottom wall periodic boundary condition. *Journal of Engineering, 20(04), pp. 99–119*. Doi:10.31026/j.eng.2014.04.07.

Ingham, 2005. Transport phenomena in porous media iii. *Elsevier*. Doi:10.1016/B978-0-08-044490-1.X5003-0.

Kalaoka, W. and Witayangkurn, S., 2012. Natural convection in a porous square enclosure with partially cooled from vertical wall. *KMITL Sci. Tech. J, 12(2), pp.180-188*.

Kamal D., Saihood R. G., 2024. Investigation on natural convection in a square porous cavity with an open side. *Journal of Engineering, 30(5), pp. 19-37*. Doi:10.31026/j.eng.2024.05.02

Kaviany, M., 1995. Principles of heat transfer in porous media. *New York, NY: Springer New York*. Doi:10.1007/978-1-4612-4254-3.

Khansila, P. and Witayangkurn, S., 2012. Visualization of natural convection in enclosure filled with porous medium by sinusoidally temperature on the one side. *Applied Mathematical Sciences, 6(97), pp. 4801–4812.*

Kim, S.J. and Choi, C.Y., 1996. Convective heat transfer in porous and overlying fluid layers heated from below. *International Journal of Heat and Mass Transfer, 39(2), pp. 319–329*. Doi:10.1016/0017-9310(95)00118-S.

Koua, B.K., Koffi, P.M.E. and Gbaha, P., 2019. Evolution of shrinkage, real density, porosity, heat and mass transfer coefficients during indirect solar drying of cocoa beans. *Journal of the Saudi Society of Agricultural Sciences, 18(1), pp. 72–82*. Doi:10.1016/j.jssas.2017.01.002.

Lock, E., Ghasemi, M., Mostofi, M. and Rasouli, V., 2012. An experimental study of permeability determination in the lab. *In: WIT Transactions on Engineering Sciences. pp. 221–230*. Doi:10.2495/PMR120201.

Mahdi A. A., Majeed M. H., Salib S. M., 2006. Numerical investigation of laminar natural convection in rectangular enclosures of porous media. *Journal of Engineering, 12(3), pp. 1666-1678.* Doi:10.31026/j.eng.2006.03.06.

Mehdy A. N., 2012. Double diffusive free convection in a packed bed square enclosure by using local thermal non-equilibrium (LTN) model. *Journal of Engineering, 18(1), pp. 121-136*. Doi:10.31026/j.eng.2012.01.09

Mashkour, M.A., Habeeb, L.J., Mohammed, H.H. and Jaber, H.J., 2013. Natural convection in a partially opened box filled with a porous medium. *Al-Qadisiyah Journal for Engineering Sciences, 6(4), pp. 400–414.*

Mohammed, N.R. and Ali, L.F., 2021. Numerical investigation for natural convection in a square enclosure with partially active thermal sides' wall. *Journal of Mechanical Engineering Research and Developments, 44(5), pp. 136–148*. https://www.researchgate.net/publication/351094105.

Nield, D.A. and Bejan, A., 2017. Convection in porous media. *Cham: Springer International Publishing*. Doi:10.1007/978-3-319-49562-0.

Pal, L., Joyce, M.K. and Fleming, P.D., 2006. A simple method for calculation of the permeability coefficient of porous media. *TAPPI JOURNAL, 5(9), pp. 10–16*.

Prakash, M., Turan, Ö.F., Li, Y. and Thorpe, G.R., 1999. A CFD study of natural convection heat and mass transfer in respiring hygroscopic porous media. *Second International Conference on CFD in the Minerals and Process Industries. pp. 157–162.*

Sathiyamoorthy, M., Basak, T., Roy, S. and Pop, I., 2007. Steady natural convection flow in a square cavity filled with a porous medium for linearly heated side wall(s). *International Journal of Heat and Mass Transfer, 50(9–10), pp. 1892–1901*. Doi:10.1016/J.IJHEATMASSTRANSFER.2006.10.010.

Straughan, 2008. Stability and wave motion in porous media. *New York, NY: Springer New York*. Doi:10.1007/978-0-387-76543-3.

Vafai, K. ed., 2015. Handbook of porous media. *CRC Press.* Doi:10.1201/b18614.

Xu, S., Chen, L., Gong, M., Hu, X., Zhang, X. and Zhou, Z., 2017. Characterization and engineering application of a novel ceramic composite insulation material. *Composites Part B: Engineering, 111, pp. 143–147*. Doi:10.1016/J.COMPOSITESB.2016.12.010.

Yazdchi, K., Srivastava, S. and Luding, S., 2011. on the validity of the carman-kozeny equation in random fibrous media. *II International Conference on Particle-based Methods – Fundamentals and Applications PARTICLES 2011, pp. 264–273*. http://www.utwente.nl/ctw/msm/.

Yoon, H.S., Ha, M.Y., Kim, B.S. and Yu, D.H., 2009. Effect of the position of a circular cylinder in a square enclosure on natural convection at Rayleigh number of 107. *Physics of Fluids, 21(4), P.047101*. Doi:10.1063/1.3112735.

Fouad J. Zachi, Luma F. Ali, 2023. Experimental study of natural convection heat transfer on an enclosure partially filled porous medium heated from below by constant heat flux. *AIP Conf. Proc., 2651 (1)*. Doi:10.1063/5.0130674.